Intrinsic gray-matter connectivity of the brain in adults with autism spectrum disorder

Christine Ecker[a,1,2], Lisa Ronan[b,1], Yue Feng[a], Eileen Daly[a], Clodagh Murphy[a], Cedric E. Ginestet[c], Michael Brammer[c], Paul C. Fletcher[b], Edward T. Bullmore[b], John Suckling[b], Simon Baron-Cohen[d], Steve Williams[c], Eva Loth[a], MRC AIMS Consortium[3], and Declan G. M. Murphy[a]

[a]Sackler Institute for Translational Neurodevelopment, Department of Forensic and Neurodevelopmental Sciences, Institute of Psychiatry, King's College London, London SE5 8AF, United Kingdom; [b]Department of Psychiatry, Cambridge and Peterborough Foundation Trust, University of Cambridge, Cambridge CB2 0SZ, United Kingdom; [c]Centre for Neuroimaging Sciences, Institute of Psychiatry, King's College London, London SE5 8AF, United Kingdom; and [d]Autism Research Centre, Department of Psychiatry, University of Cambridge, Cambridge CB2 8AH, United Kingdom

Autism spectrum disorders (ASD) are a group of neurodevelopmental conditions that are accompanied by atypical brain connectivity. So far, in vivo evidence for atypical structural brain connectivity in ASD has mainly been based on neuroimaging studies of cortical white matter. However, genetic studies suggest that abnormal connectivity in ASD may also affect neural connections within the cortical gray matter. Such intrinsic gray-matter connections are inherently more difficult to describe in vivo but may be inferred from a variety of surface-based geometric features that can be measured using magnetic resonance imaging. Here, we present a neuroimaging study that examines the intrinsic cortico-cortical connectivity of the brain in ASD using measures of "cortical separation distances" to assess the global and local intrinsic "wiring costs" of the cortex (i.e., estimated length of horizontal connections required to wire the cortex within the cortical sheet). In a sample of 68 adults with ASD and matched controls, we observed significantly reduced intrinsic wiring costs of cortex in ASD, both globally and locally. Differences in global and local wiring cost were predominantly observed in fronto-temporal regions and also significantly predicted the severity of social and repetitive symptoms (respectively). Our study confirms that atypical cortico-cortical "connectivity" in ASD is not restricted to the development of white-matter connections but may also affect the intrinsic gray-matter architecture (and connectivity) within the cortical sheet. Thus, the atypical connectivity of the brain in ASD is complex, affecting both gray and white matter, and forms part of the core neural substrates underlying autistic symptoms.

brain structure | gyrification | morphometry

Autism spectrum disorders (ASDs) are a group of neurodevelopmental conditions characterized by impaired social communication, social reciprocity, and repetitive/stereotypic behavior (1). There is consensus that ASD is accompanied by developmental differences in brain anatomy and connectivity (2). However, the specific neurobiological substrate of ASD remains elusive.

Neuroimaging evidence suggests that ASD is accompanied by anatomical differences in several large-scale neurocognitive networks (3), which typically include the cerebellum (4), the amygdala–hippocampal complex (5), fronto-temporal regions (6), and the caudate nuclei (7). These gross-anatomical abnormalities are likely to reflect differences in the cytoarchitectonic make-up of individual brain regions in ASD, as can be observed in postmortem studies. For instance, individuals with ASD may have a reduced size, but increased number, of minicolumns (8), which could underpin differences in cortical surface area (9, 10). Also, individuals with ASD may have an excess number of neurons in some brain regions (11), which in turn may affect measures of cortical thickness (9, 12). Therefore, different morphometric features of the cortical surface provide proxy measures of various aspects of local gray-matter architecture. However, currently there is a lack of imaging markers that can be used to explore gray-matter neuroanatomy as a connected neural system.

The development of such biomarkers is important because increasing evidence suggests that ASD is accompanied by atypical structural "brain connectivity" within the wider neural systems mediating autistic symptoms and traits (13–15). So far, the notion of abnormal anatomical connectivity in ASD is mainly based on neuroimaging studies examining white-matter differences using voxel-based morphometry (e.g., ref. 6) or diffusion tensor imaging (DTI) (e.g., refs. 16 and 17)). However, genetic and molecular studies suggest that abnormal neural connectivity in ASD may not be restricted to white-matter connectivity of the brain but also affect direct synaptic connections within cortical gray matter. For example, many of the genes and/or copy number variants (CNVs) associated with ASD encode for genes involved in cell adhesion, synaptogenesis, and maturation (reviewed in refs. 5, 6, and 18). One would therefore expect that ASD is also associated with differences in local cortico-cortical circuits that do not communicate via white matter (i.e., those "intrinsic" to the cortical sheet).

Such intrinsic cortico-cortical connections have been well described in histological studies and generally denote connections running parallel to the cortical surface (Fig. 1A). As such, intrinsic connections are confined to the cortical gray matter and should be distinguished from extrinsic connections that pass through white matter and terminate in other cortical regions (e.g., U-fibers or interhemispheric connections) (19). For example, Lewis et al. (20) reported the existence of excitatory intrinsic long-range axon collaterals in the prefrontal cortex, which can extend up to 4–5 millimeters along the cortical surface (see also ref. 21). Intrinsic connections have also been documented in other regions of the brain (e.g., visual, motor, and somatosensory cortices) (22) and may include components of the inhibitory cortical circuitry (e.g., wide-arbor basket cells) (23). Intrinsic connections are therefore an integral part of the horizontal (i.e., lateral) gray-matter architecture of the cortex, and their development has therefore been closely related to a variety of surface-based geometric features, including surface area (10), cortical separation distances (24), and Gaussian curvature (25). These measures are also known as
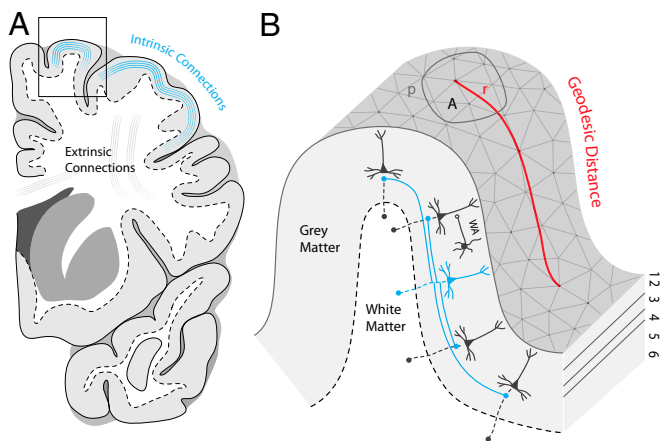
Fig. 1. (A) Schematic diagram illustrating the intrinsic horizontal connectivity of the cortex including long-range intrinsic axon collaterals of pyramidal neurons (cyan) and terminals of wide-arbor (WA) inhibitory basket cells. (B) Geodesic mesh consisting of points (i.e., vertices) characterizing the cortical surface. The geodesic distance (marked in red) is the shortest path along the surface that connects two surface points. Circle indicates geodesic circle of area A, radius r, and perimeter p.

intrinsic geometric measures as they are a property of the surface itself and are thus independent of how the cortex is embedded or "folded" in 3D space (24, 26). Therefore, given the putative link between cortical surface morphometry and intrinsic corticocortical connectivity, such novel geometric measures are particularly suited to investigate the complex cortical anatomy of ASD in vivo.

In the present study, we used these surface-based geometric features to investigate the intrinsic cortical organization of the brain in adults with ASD and healthy controls. The intrinsic organization of the cortex was assessed using measures of "cortical separation distances," which represent the length of the shortest path(s) linking two points on the cortical surface (i.e., geodesic distances) (Fig. 1B). These distances (also known as the geodesics) travel along the cortical surface, and in parallel to intrinsic horizontal connections, and may therefore be used for estimating the intrinsic "wiring cost" of the cortex (i.e., estimated minimum length of horizontal connections required to wire regions within the cortical sheet) (24).

For each vertex, wiring costs were firstly estimated on the global level using so-called "mean separation distances" (MSDs), which indicate the average geodesic distance from a vertex to the rest of the surface. Subsequently, intrinsic wiring costs were assessed on the local level by estimating separation distances within a circular cortical patch or "geodesic circle" covering a given proportion of the cortical surface (Fig. 1B). Here, the radius of the circle was used to assess "intraareal" wiring cost whereas the perimeter of the circle was used to measure the "interareal" wiring cost (24). Based on the previous notion of local overconnectivity in ASD (27), it was expected that individuals with ASD display reduced intraareal wiring costs, predominantly in fronto-temporal regions, and that both global and local measures of intrinsic connections would be associated with variations in symptom severity.

Results

Subject Demographics and Global Brain Measures. There were no significant differences between individuals with ASD and controls in age [t (66) = 1.65, P = 0.10] or full scale IQ (FSIQ) [t (66) = 1.49, P = 0.14] (Table S1). There were also no significant between-group differences in total brain volume [t (66) = −0.42, P = 0.67] or total surface area [t (66) = −1.36, P = 0.17].

Differences in MSDs. Overall, there was considerable variation in MSDs across the cortical surface (Fig. 2 A and B). As expected,

maximally separated vertices were located close to the frontal and occipital pole whereas points of minimal separation were observed close to the junction of the sylvian fissure and the central sulcus.

There were no brain regions in which individuals with ASD had a significant increase in MSD relative to controls. However, individuals with ASD had significantly lower MSDs in several significant clusters in the left hemisphere, including the (i) pre- and postcentral gyrus and primary motor cortex [Brodmann area (BA) 4], somatosensory cortex (BA 1/2/3), and posterior parietal cortex (BA 5/7); (ii) anterior and middle temporal lobe (BA 20/21/38); and (iii) orbitofrontal prefrontal cortex (BA 10/11). We also observed reduced MSDs in ASD in the right temporo-parietal junction (BA 39) (Fig. 2C).

Within the ASD group, lower MSDs were primarily correlated with the more severe Autism Diagnostic Interview-Revised (ADI-R) scores in the repetitive domain (Fig. 2D) in the (i) right inferior temporal lobe (BA 20/37), the right somatosensory and central gyri, and in the right orbitofrontal cortex (BA 10); also (ii) the left and right temporo-parietal junction (BA 39/40). There were no significant correlations between MSDs and the ADI-R social/communication domains using P < 0.01 (see Fig. S1 for behavioral correlations at P < 0.05); nor with the severity of current autistic symptoms as measured by the Autism Diagnostic Observation Schedule (ADOS).

Differences in Radius and Perimeter Function. Figure 3 A and D shows the intraareal and interareal wiring-cost functions averaged across controls (at a scale of 5%), which are also referred to as the radius function and perimeter function, respectively.

There were no brain regions in which the radius function of the cortex was significantly increased in individuals with ASD. However, in ASD, we found significantly reduced radii (i.e., within-path distances) in the (i) bilateral anterior and medial temporal lobe (BA 21/22); (ii) bilateral dorsolateral prefrontal cortices (BA
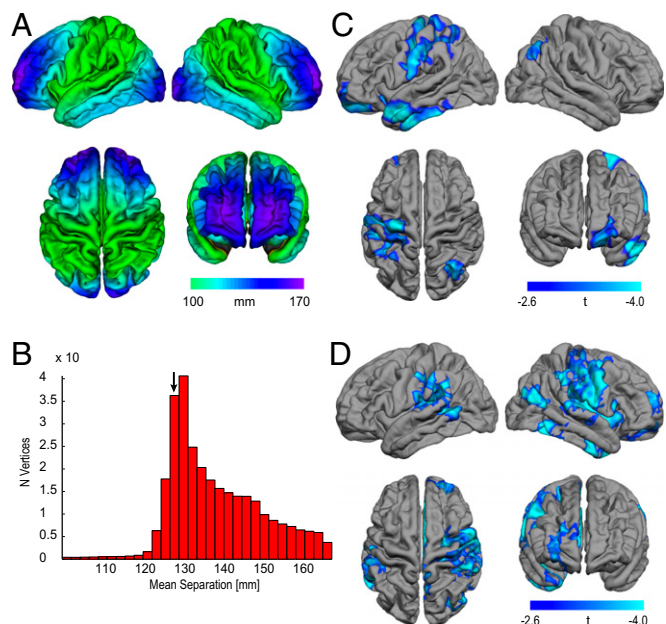
Fig. 2. (A) MSDs for points on the cortical surface, averaged across controls. (B) Distribution of MSDs across the cortical surface. The arrow indicates the average of the distribution (i.e., "mean geodesic"). (C) Random-field, theory-based, cluster-corrected (P < 0.01) difference map showing significantly reduced MSDs in ASD relative to controls. (D) Clusters of significant negative correlations between MSDs and the repetitive domain of the ADI-R within the ASD group (RFT-based, cluster-corrected, P < 0.01). r_{neg}, negative correlation coefficient; t, statistical test parameter for correlation coefficient.

SYSTEMS BIOLOGY
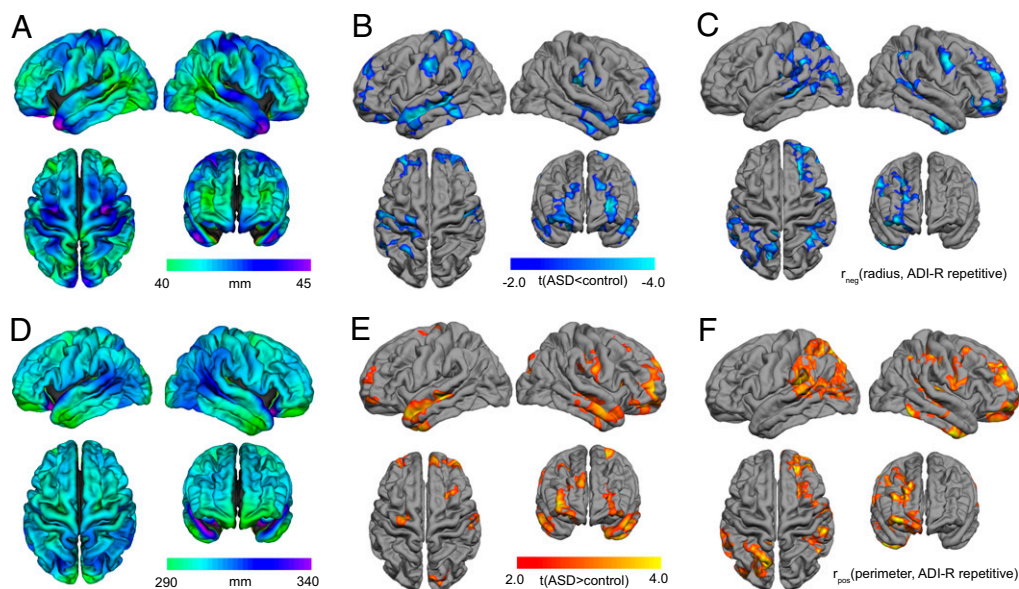
Fig. 3. (*A*) Intraareal wiring-cost function (referred to as the radius function) of the cortex at a scale of 5% averaged across controls. (*B*) Random-field, theory-based, cluster-corrected (*P* < 0.05) difference map indicating regions with reduced radii in ASD relative to controls. (*C*) Clusters of significant negative correlations (*P* < 0.05) between radius function and the severity of autistic symptoms in the repetitive domain. (*D*) Interareal wiring-cost function (referred to as the perimeter function) averaged across controls at a scale of 5%. (*E*) Clusters (RFT-based, cluster corrected, *P* < 0.05) with enhanced perimeters in ASD relative to controls. (*F*) Clusters (RFT-based, cluster-corrected, *P* < 0.05) of significant positive correlations between perimeter and the severity of autistic symptoms in the repetitive domain.

10/11); (*iii*) bilateral somatosensory cortex/postcentral gyrus (BA 1–3); and (*iv*) left posterior parietal cortex (BA 5/7) and temporo-parietal junction (BA 39) (Fig. 3*B*; see Table S2 for details).

There were no brain regions in which the perimeter function of the cortex was significantly reduced in individuals with ASD. However, we found significantly increased perimeters in the bilateral (*i*) temporal lobes (BA 20/21/38); (*ii*) ventro-lateral prefrontal cortex (BA 10/11); and (*iii*) precentral gyrus (BA 4/6) (Fig. 3*E*, Table S2).

Within the ASD group, lower radii and larger perimeters were predominantly correlated with more severe ADI-R scores in the repetitive domain (Fig. 3 *C* and *F*), and (to a less extent) with more severe social/communication symptoms (Fig. S1). There we no significant correlations with the ADOS total.

Scale Sensitivity and Robustness of the Results. Further examinations indicated that results were independent of the cortical tessellation. As expected, the observed between-group differences in all three investigated measures were most prominent on the native high-resolution cortical mesh and gradually decayed with increasing levels of mesh simplification (Fig. 4). Overall, the pattern of differences remained stable when comparing the original mesh with the standardized and down-sampled mesh with 40,962 vertices (first degree decimation), indicating the validity and robustness of our finding across differences in mesh patterning of the same underlying neuroanatomy. The results were also robust across different smoothing filters and using the down-sampled cortical "midsurfaces" (Figs. S2 and S3). Local differences were more sensitive to the level of mesh simplification than global differences, suggesting that differences in intrinsic wiring costs are caused by morphological variations in surface anatomy, rather than reflecting differences due to the actual mesh patterning (e.g., density/number of vertices characterizing the cortical surface).

Discussion

Here, we examined the intrinsic morphology of the brain in adults with ASD in vivo. Measures of cortical separation distances (MSDs) were used to assess the global and local intrinsic wiring costs of the cortex indicating the estimated minimal length of intrinsic connections required to wire the cortex within the cortical sheet. The intrinsic organization of the brain in ASD differed significantly from controls in both global and local wiring costs. Further, global and local wiring costs were significantly correlated with severity of autistic symptoms, notably in the tendency to engage in repetitive behaviors. Our study suggests that atypical

cortico-cortical "connectivity" in ASD may not be restricted to extrinsic white-matter connections but may also affect the intrinsic neural architecture and connectivity of the brain within cortical gray matter, which may impact on specific autistic symptoms and traits.

It has previously been noted that the brain is both intrinsically and extrinsically connected (20). Extrinsic white-matter connectivity has been extensively studied in ASD using a variety of diffusion
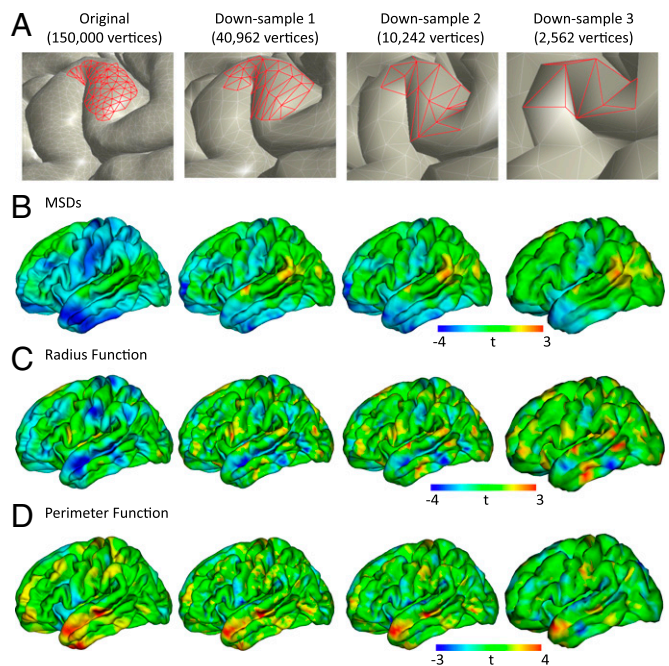
Fig. 4. (*A*) Cortical mesh patterning of the original high-resolution pial surface and of three standard templates with decreasing levels of resolution. The vertices delineated are roughly within the same location and illustrate the degree of detail lost at each successive iteration. (*B*–*D*) Difference maps (t statistic) between individuals with ASD and controls for mean separation distances (*B*), intraareal wiring costs (*C*), and interareal wiring costs (*D*). Negative t values (green to blue) indicate smaller parameter values in ASD relative to controls whereas positive t values (green to red) indicate larger parameter values in ASD.

tensor imaging (DTI) and/or voxel-based morphometry (VBM) measures, which broadly assess differences in white-matter volume and integrity (7, 17, 28). Less attention has been paid to the exploration of intrinsic cortico-cortical connections, which are confined to the cortical gray matter. Although these connections can extend up to a few millimeters (19, 21), intrinsic connections are difficult to measure in vivo as they are not explicitly quantifiable by conventional measures of brain volume or cortical thickness. Intrinsic connections are, however, well documented in the in vitro literature and have previously been implicated in other neurodevelopmental/neuropsychiatric conditions, such as schizophrenia (29–31), where more postmortem data are currently available to allow histological characterization relative to ASD. We therefore used a surface-based approach to brain morphometry (24) to investigate the horizontal organization of the cortex in ASD.

Intrinsic wiring costs of the cortex were initially estimated globally based on MSDs and subsequently compared between groups. MSDs indicate the average length of connections required to wire each vertex to the rest of the cortex along the cortical surface and are thus independent of the individual's pattern of cortical folding. As assessed here, wiring costs do not represent the actual length of axonal connections but are indicative of the intrinsic "wiring potential" of a brain region (i.e., reduced costs may facilitate the formation of intrinsic cortico-cortical circuits). As such, intrinsic measures reflect the actual intrinsic architecture of the brain, which may differ across different regions and may also include different neural components characterizing the lateral (i.e., horizontal) architecture of the cortex (30, 32).

We found that individuals with ASD had significantly reduced MSDs in several fronto-temporal and central regions and that these differences were observed in the absence of a significant difference in overall volume of brain, gray matter, and white matter or in total surface area. Thus, reduced cortico-cortical wiring costs (and potentially shorter intrinsic connections) in ASD may arise from a fundamentally different morphology of the brain (or vice versa), rather than simply a difference in brain size. Atypical cortical morphology has previously been reported in ASD (33–36) and may be more "complex" than in controls (37, 38). Our finding of reduced MSDs further supports the hypothesis that increased geometric complexity may underpin the development of shorter cortico-cortical fibers at the expense of longer connections (25, 39). If so, a relative imbalance of short- to long-range cortical projections most likely also affects the way information is processed in the brain in ASD and may favor what some have suggested as a preference for local over global information (e.g., ref. 40). A preference for local over global connections might also explain the reduced degree of functional brain connectivity in the large-scale neurocognitive networks underlying ASD, which has been noted in many prior studies (e.g., refs. 41–43).

These differences in basic information processing may also impact on wider autistic symptoms. For example we found that, within the ASD group, MSDs in several prefrontal regions and in the somatosensory, motor, and premotor cortex were significantly correlated with the severity of repetitive autistic symptoms. We also found that MSDs in several regions of the "social brain" network (44) (e.g., anterior temporal lobe, fusiform gyrus) were significantly negatively correlated with the severity of social autistic symptoms. These are also regions that have previously been suggested to underpin (respectively) theory-of-mind deficits (e.g., ref. 45), abnormal activation by faces and biological motion (e.g., refs. 46 and 47). Thus, the organization of specific regions on the cortical surface may modulate symptom severity in some (but not all) autistic symptom domains.

Differences in intrinsic geometry of the cortex have previously also been related to the density of neural units defining the surface architecture of individual cortical regions (25, 30). Theoretically (Fig. S4), if the MSD of a point is high, then that point is relatively more isolated (i.e., in a low-density environment) compared with a point with a low MSD (i.e., in a high-density environment). Thus, comparing MSD distributions across groups may reveal regions that have relatively greater or lesser density of underlying "surface

units." These units are not necessarily synonymous with the number of vertices characterizing the cortical surface as cortical distances were measured using an algorithm that provides "subgrid" resolution and the resulting path lengths are close approximations to the true shortest paths, rather than being confined to run along the edges (i.e., direct connection) between two vertices. In addition, the observed pattern of differences was stable across different mesh patterning and gradually decayed with increasing levels of mesh simplification. Thus, we argue that MSDs are more closely related to the number of underlying neural units defining the morphology of the cortical surface. For example, many regions with significantly reduced MSDs (e.g., BA 3–4, 9, and 21–22) overlap with those that have previously been reported to have an increased minicolumn density in ASD, and decreased peripheral neuropil space (PNS) (48, 49). Thus, our findings suggest that differences in MSDs may be closely related to the density of cortical minicolumns, and that minicolumns may be more unevenly distributed (and so more dense) in some regions relative to others.

An uneven distribution of surface units (e.g., minicolumns) most likely arises as a consequence of nonuniform surface expansion during development, which is commensurate with a differential decrease in neuronal density and an increase in intercellular spacing (25, 32). For example, it has previously been demonstrated that some regions expand earlier and to a higher extent than others in typical brain development, and such differential expansion will also affect the distances between regions on the cortical surface (e.g., ref. 50). In ASD, the degree of cortical surface expansion may be increased (i.e., earlier, more rapid growth during childhood) (e.g., refs. 51 and 52) and may be more variable (i.e., nonuniform) across the brain—with frontal and temporal lobes perhaps being more affected than occipital and parietal lobes (e.g., ref. 53). Such differential overgrowth in ASD will affect both overall size of the cortex and the way the brain is organized and "wired" (27). Our results, and the work of others, therefore suggest that measures of intrinsic geometry might also be used as an in vivo neuroimaging marker for nonuniform cortical expansion during development (25). In adults, it is often difficult to determine whether between-group differences result from (*i*) the primary pathology, (*ii*) a different neurodevelopmental trajectory, or (*iii*) general compensatory mechanisms unrelated to the primary pathology. We found, however, that measures of intrinsic connectivity primarily correlated with ADI-R scores reflecting symptom severity during childhood but not with ADOS scores (i.e., current symptoms). This observation further supports the notion that differences in intrinsic connectivity in adults with ASD may reflect the end result of an atypical trajectory of brain development rather than simply reflecting general compensatory mechanisms in later life.

Differences in wiring costs were also observed on the local level, where we found reductions in radius function and increases in perimeter function of the cortex in ASD. Griffin (24) suggests that the relationship between intrinsic geometry and connectivity of the cortex may also be considered in terms of intra- and interareal wiring costs, which can be assessed using the radius function and perimeter function, respectively. Biologically, the cost of connections is related to their number and their length. The length of connections is restrained by the radius function—where smaller radii facilitate intraareal wiring (i.e., smaller "within-path" distances). The number of connections, on the other hand, is constrained by the perimeter function where larger perimeters facilitate the development of interareal connections (*SI Text*). Thus, our finding of reduced within-path distances combined with increased perimeter size in ASD indicates enhanced intrinsic cortico-cortical wiring within and between areas, which may lead to locally "overconnected" regions that have previously been suggested to underpin ASD (e.g., ref. 27).

For all geometrics, there is a positive relationship between radius function and perimeter function. However, in our results (Fig. 3), we see that many regions with reduced radius function also show an increased perimeter. This can be explained by the fact that different geometries have different radius-to-perimeter ratios. Although the ratio is always positive, it is determined by the degree

of curvature. For example, the increase in perimeter relative to radius is less in positive curvature compared with Euclidean geometry whereas, in negative curvature, the perimeter increases exponentially relative to the radius. Thus, depending on different geometries, a patch of uniform area may be achieved by either an increased or decreased ratio of radius to perimeter. Our results therefore further suggest that the brain has negative curvature, which supports previous observations using alternative measures of intrinsic cortical morphometry (25, 30).

The molecular and genetic mechanisms underlying the atypical expansion and wiring of the cortex in ASD remain largely unknown. From a neurodevelopmental perspective, the total number of minicolumns characterizing the cortical surface is set during the stage of germinal cell divisions (54), which may suggest that cortical expansion in ASD could be related to an increase in duration of this stage of gestation, as well as the longevity of germinal cells. Furthermore, the time window of brain overgrowth in ASD coincides with the period when processes of synaptogenesis, dendritic growth, and myelination are at their peak (reviewed in ref. 55). Evidence for atypical synaptic functioning and brain connectivity in ASD also comes from a variety of recent genetic investigations. For example, several CNVs that have recently been associated with ASD encode genes involved in synaptogenesis and neuronal differentiation (reviewed in ref. 56). These genetic variants include genes encoding for cell adhesion molecules (e.g., neuroligins and neurexins) that play key roles in the formation and consolidation of synaptic contacts (e.g., ref. 57). These specific molecular components of the neural architecture are naturally inaccessible in the human brain in vivo. However, such studies clearly highlight the need for developing neuroimaging markers for cortico-cortical graymatter development, such as the measures introduced in the present study, which may be used to guide future genetic (and histological) investigations into the complex etiology of ASD.

Materials and Methods

Participants. Thirty-four male right-handed adults with ASD and 34 matched typical male controls aged 18–43 y were recruited by advertisement and assessed at the Institute of Psychiatry, London (Table S1). Exclusion criteria included a history of major psychiatric disorder (e.g., psychosis), head injury, genetic disorder associated with autism (e.g., fragile-X syndrome, tuberous sclerosis), or any other medical condition affecting brain function (e.g., epilepsy). We excluded participants on antipsychotic medication, mood stabilizers, or benzodiazepines. All participants with ASD were diagnosed according to International Classification of Diseases (ICD)-10 research criteria and confirmed using the Autism Diagnostic Interview-Revised (ADI-R) (58). All cases reached the diagnostic algorithm cutoffs for adults in the three domains of the ADI-R although failure to reach cutoff in one domain by one point was permitted.

Current symptoms were assessed using the Autism Diagnostic Observation Schedule (ADOS) (59) and were not used as inclusion criteria. Overall, intellectual ability was assessed using the Wechsler Abbreviated Scale of Intelligence (WASI) (60). All participants fell within the high-functioning range on the spectrum defined by a Full Scale IQ greater than 70. All participants gave informed written consent in accordance with ethics approval by the National Research Ethics Committee, Suffolk, United Kingdom.

MRI Data Acquisition. Scanning took place at the Institute of Psychiatry, London, using a 3T GE Signa System (General-Electric). Details of the acquisition protocol have been previously described elsewhere (3, 61). Briefly, quantitative T_1-maps were used to derive high-resolution structural T_1-weighted inversion-recovery images, with $1 \times 1 \times 1$ mm resolution, a $256 \times 256 \times 176$ matrix, repetition time = 1,800 ms, inversion time = 50 ms, flip angle = 20°, and field-of-view = 5 cm. These images were subsequently used for surface reconstruction.

Cortical Reconstruction Using FreeSurfer. Scans were initially screened by a radiologist to exclude clinically significant abnormalities and to assess the existence of movement. Scans of insufficient quality were excluded from the analysis. The FreeSurfer software package (vFS5.1 release) was used to derive models of the cortical surface in each T_1-weighted image. These wellvalidated and fully automated procedures have been extensively described elsewhere (e.g., refs. 62–66). In brief, a single filled white-matter volume was generated for each hemisphere after intensity normalization, the removal of

extracerebral tissue, and image segmentation using a connected components algorithm. A triangular surface tessellation was then generated for each white-matter volume by fitting a deformable template, resulting in a cortical mesh for white and gray/pial (i.e., outer) surface with ~150,000 vertices (i.e., points) per hemisphere. No manual edits were necessary. The pial surfaces were subsequently used for distance computations.

Estimation of Global Intrinsic Wiring Costs: MSDs. Cortical separation distances were defined as the length of the shortest path(s) linking two vertices on the cortical surface (i.e., "geodesic distance" between two points) (Fig. 1A, Fig. S5). Distances computed along the cortical surface are unaffected by how the surface is embedded in 3D space and are therefore intrinsic to the surface itself (24). For example, the distance between two points on a sheet of paper remains the same regardless of whether the sheet is folded or unfolded. Thus, intrinsic measures are distinguished from extrinsic features such as cortical folding, which affect the 3D alignment of the cortex but does not alter distances between surface points (25, 30).

First, geodesic distances between each vertex and all other locations on the cortical surface were computed using the "Fast-Marching-Toolbox" for Matlab (R2011b; The Mathworks) (67, 68) (see Fig. S5 for details). Distance computation resulted in an n by n matrix of distances D with zeros values in the diagonal, where n equals the number of vertices on each surface. The $nx1$ row/column means of D equaled the MSD for each vertex, i.e., average geodesic distance from vertex to the rest of the surface. Because MSDs travel in parallel to intrinsic axonal connections, MSDs were tentatively described as capturing the global intrinsic wiring cost of the surface (i.e., estimated length of horizontal connections required to wire the cortex within the cortical sheet) (24).

Estimation of Local Intrinsic Wiring Costs: Radius Function and Perimeter Function. Local intrinsic wiring costs were estimated on the basis of geodesic circles (i.e., circular patches) superimposed onto the cortical surface (Fig. 1B). A geodesic circle of radius r centered at a point (i.e., vertex) p is that proportion of the surface that lies within a geodesic distance r of the point p. Local wiring costs can therefore be assessed at a range of scales expressed as a proportion of the total (see Fig. S6 for between-group difference in vertex-based measures of surface area). Here, we used a scale of 5%. The radius of the circle characterizes the "radius function" of the cortex, which can be used to estimate the intraareal intrinsic wiring cost at a given vertex (i.e., radius indicates the minimum length of connections required to wire a vertex with regions inside the patch) (24). The perimeter of the circle characterizes the perimeter function or circumference function of the cortex indicating the intrinsic interareal wiring costs (i.e., costs associated with wiring this point to adjacent areas outside the patch) (SI Text).

Last, to test for scale sensitivity and robustness of the results, each subject's original pial surface was also mapped to standard templates with three different levels of resolution (decreasing resolution: 40,962, 10,242, and 2,562 vertices, respectively) included in the FreeSurfer vFS5.1 release. The mesh simplification/standardization did not deform the shape of an individual's surfaces; rather it generated a new surface with less numerous vertices and the same number of vertices across subjects (Fig. 4A). Separation distances were then recomputed on the down-sampled surfaces for each level of resolution to assess the validity of the observed between-group differences. In addition, we examined the robustness of the results on cortical midsurfaces (i.e., "mean surface" between pial- and white-matter surface), and using different smoothing filters (2, 5, and 10 mm).

Statistical Comparison Between ASD and Neurotypicals. To improve the ability to detect population changes, each parameter was smoothed using a 2-mm surface-based smoothing kernel before statistical analysis. Statistical analysis was conducted using the SurfStat toolbox (www.math.mcgill.ca/keith/surfstat/) for Matlab (R2010b; The Mathworks). Parameter estimates for dependent variables y_i (MSDs, wiring costs) and the main effect of group G_i were estimated by regression of a general linear model at each vertex i, with total surface area S_i as covariate:

$$y_i = \beta_0 + \beta_1\,G_i + \beta_2\,S_i + \varepsilon_i,$$

where ε is the residual error. Between-group differences were estimated from the coefficient β_1 normalized by the corresponding SE. The relationship between intrinsic features and measures of symptom severity (ADI-R subscores, ADOS total) was assessed using linear regression while covarying for total surface area. Corrections for multiple comparisons across the whole brain were performed using random field theory (RFT)-based cluster analysis for nonisotropic images using a $P < 0.05$ (2-tailed) cluster-significance threshold

for significant between-group differences and behavioral correlations in local features (radius/perimeter functions) (69). For MSDs, a more conservative cluster-corrected threshold of $P < 0.01$ was used as effect sizes and cluster sizes were considerably larger than observed in local features. Between-group differences in global brain measures were examined using independent samples t tests.

1. Wing L (1997) The autistic spectrum. *Lancet* 350(9093):1761–1766.
2. Amaral DG, Schumann CM, Nordahl CW (2008) Neuroanatomy of autism. *Trends Neurosci* 31(3):137–145.
3. Ecker C, et al.; MRC AIMS Consortium (2012) Brain anatomy and its relationship to behavior in adults with autism spectrum disorder: A multicenter magnetic resonance imaging study. *Arch Gen Psychiatry* 69(2):195–209.
4. Courchesne E, Yeung-Courchesne R, Press GA, Hesselink JR, Jernigan TL (1988) Hypoplasia of cerebellar vermal lobules VI and VII in autism. *N Engl J Med* 318(21):1349–1354.
5. Abell F, et al. (1999) The neuroanatomy of autism: A voxel-based whole brain analysis of structural scans. *Neuroreport* 10(8):1647–1651.
6. McAlonan GM, et al. (2005) Mapping the brain in autism: A voxel-based MRI study of volumetric differences and intercorrelations in autism. *Brain* 128(Pt 2):268–276.
7. Langen M, et al. (2012) Fronto-striatal circuitry and inhibitory control in autism: Findings from diffusion tensor imaging tractography. *Cortex* 48(2):183–193.
8. Casanova MF, Buxhoeveden DP, Switala AE, Roy E (2002) Neuronal density and architecture (Gray Level Index) in the brains of autistic patients. *J Child Neurol* 17(7):515–521.
9. Rakic P (1995) A small step for the cell, a giant leap for mankind: A hypothesis of neocortical expansion during evolution. *Trends Neurosci* 18(9):383–388.
10. Ecker C, et al.; MRC AIMS Consortium (2013) Brain surface anatomy in adults with autism: The relationship between surface area, cortical thickness, and autistic symptoms. *JAMA Psychiatry* 70(1):59–70.
11. Courchesne E, et al. (2011) Neuron number and size in prefrontal cortex of children with autism. *JAMA* 306(18):2001–2010.
12. Hyde KL, Samson F, Evans AC, Mottron L (2010) Neuroanatomical differences in brain areas implicated in perceptual and other core features of autism revealed by cortical thickness analysis and voxel-based morphometry. *Hum Brain Mapp* 31(4):556–566.
13. Geschwind DH, Levitt P (2007) Autism spectrum disorders: Developmental disconnection syndromes. *Curr Opin Neurobiol* 17(1):103–111.
14. Lewis JD, Elman JL (2008) Growth-related neural reorganization and the autism phenotype: A test of the hypothesis that altered brain growth leads to altered connectivity. *Dev Sci* 11(1):135–155.
15. Belmonte MK, et al. (2004) Autism and abnormal development of brain connectivity. *J Neurosci* 24(42):9228–9231.
16. Catani M, et al. (2008) Altered cerebellar feedback projections in Asperger syndrome. *Neuroimage* 41(4):1184–1191.
17. Pugliese L, et al. (2009) The anatomy of extended limbic pathways in Asperger syndrome: A preliminary diffusion tensor imaging tractography study. *Neuroimage* 47(2):427–434.
18. Abrahams BS, Geschwind DH (2010) Connecting genes to brain in the autism spectrum disorders. *Arch Neurol* 67(4):395–399.
19. Levitt JB, Lewis DA, Yoshioka T, Lund JS (1993) Topography of pyramidal neuron intrinsic connections in macaque monkey prefrontal cortex (areas 9 and 46). *J Comp Neurol* 338(3):360–376.
20. Lewis DA, Melchitzky DS, Burgos G-G (2002) Specificity in the functional architecture of primate prefrontal cortex. *J Neurocytol* 31(3-5):265–276.
21. Melchitzky DS, González-Burgos G, Barrionuevo G, Lewis DA (2001) Synaptic targets of the intrinsic axon collaterals of supragranular pyramidal neurons in monkey prefrontal cortex. *J Comp Neurol* 430(2):209–221.
22. Lund JS, Yoshioka T, Levitt JB (1993) Comparison of intrinsic connectivity in different areas of macaque monkey cerebral cortex. *Cereb Cortex* 3(2):148–162.
23. Lund JS, Wu CQ (1997) Local circuit neurons of macaque monkey striate cortex. IV. Neurons of laminae 1-3A. *J Comp Neurol* 384(1):109–126.
24. Griffin LD (1994) The intrinsic geometry of the cerebral cortex. *J Theor Biol* 166(3):261–273.
25. Ronan L, et al. (2011) Intrinsic curvature: A marker of millimeter-scale tangential cortico-cortical connectivity? *Int J Neural Syst* 21(5):351–366.
26. Van Essen DC, Maunsell JH (1980) Two-dimensional maps of the cerebral cortex. *J Comp Neurol* 191(2):255–281.
27. Courchesne E, Pierce K (2005) Why the frontal cortex in autism might be talking only to itself: Local over-connectivity but long-distance disconnection. *Curr Opin Neurobiol* 15(2):225–230.
28. Barnea-Goraly N, et al. (2004) White matter structure in autism: Preliminary evidence from diffusion tensor imaging. *Biol Psychiatry* 55(3):323–326.
29. Lewis DA, González-Burgos G (2008) Neuroplasticity of neocortical circuits in schizophrenia. *Neuropsychopharmacology* 33(1):141–165.
30. Ronan L, et al. (2012) Consistency and interpretation of changes in millimeter-scale cortical intrinsic curvature across three independent datasets in schizophrenia. *Neuroimage* 63(1):611–621.
31. Lewis DA (2009) Neuroplasticity of excitatory and inhibitory cortical circuits in schizophrenia. *Dialogues Clin Neurosci* 11(3):269–280.
32. Ronan L, et al. (2013) Differential Tangential Expansion as a Mechanism for Cortical Gyrification. *Cereb Cortex*.
33. Piven J, et al. (1990) Magnetic resonance imaging evidence for a defect of cerebral cortical development in autism. *Am J Psychiatry* 147(6):734–739.
34. Hardan AY, Jou RJ, Keshavan MS, Varma R, Minshew NJ (2004) Increased frontal cortical folding in autism: A preliminary MRI study. *Psychiatry Res* 131(3):263–268.
35. Nordahl CW, et al. (2007) Cortical folding abnormalities in autism revealed by surface-based morphometry. *J Neurosci* 27(43):11725–11735.
36. Levitt JG, et al. (2003) Cortical sulcal maps in autism. *Cereb Cortex* 13(7):728–735.
37. Nitzken M, et al. (2011) 3D shape analysis of the brain cortex with application to autism. *Proceedings of the IEEE International Symposium on Biomedical Imaging* (IEEE, Washington, DC), pp 1847–1850.
38. Thompson PM, et al. (2005) Abnormal cortical complexity and thickness profiles mapped in Williams syndrome. *J Neurosci* 25(16):4146–4158.
39. Casanova MF, et al. (2009) Reduced gyral window and corpus callosum size in autism: Possible macroscopic correlates of a minicolumnopathy. *J Autism Dev Disord* 39(5):751–764.
40. Happé F, Frith U (2006) The weak coherence account: Detail-focused cognitive style in autism spectrum disorders. *J Autism Dev Disord* 36(1):5–25.
41. Anderson JS, et al. (2011) Decreased interhemispheric functional connectivity in autism. *Cereb Cortex* 21(5):1134–1146.
42. Gotts SJ, et al. (2012) Fractionation of social brain circuits in autism spectrum disorders. *Brain* 135(Pt 9):2711–2725.
43. Just MA, Cherkassky VL, Keller TA, Kana RK, Minshew NJ (2007) Functional and anatomical cortical underconnectivity in autism: Evidence from an FMRI study of an executive function task and corpus callosum morphometry. *Cereb Cortex* 17(4):951–961.
44. Blakemore S-J (2008) The social brain in adolescence. *Nat Rev Neurosci* 9(4):267–277.
45. Castelli F, Frith C, Happé F, Frith U (2002) Autism, Asperger syndrome and brain mechanisms for the attribution of mental states to animated shapes. *Brain* 125(Pt 8):1839–1849.
46. Pelphrey KA, et al. (2003) Brain activity evoked by the perception of human walking: Controlling for meaningful coherent motion. *J Neurosci* 23(17):6819–6825.
47. Allison T, Puce A, McCarthy G (2000) Social perception from visual cues: Role of the STS region. *Trends Cogn Sci* 4(7):267–278.
48. Casanova MF, Buxhoeveden DP, Brown C (2002) Clinical and macroscopic correlates of minicolumnar pathology in autism. *J Child Neurol* 17(9):692–695.
49. Casanova MF, et al. (2006) Minicolumnar abnormalities in autism. *Acta Neuropathol* 112(3):287–303.
50. Hill J, et al. (2010) Similar patterns of cortical expansion during human development and evolution. *Proc Natl Acad Sci USA* 107(29):13135–13140.
51. Courchesne E, et al. (2001) Unusual brain growth patterns in early life in patients with autistic disorder: An MRI study. *Neurology* 57(2):245–254.
52. Hazlett HC, et al. (2011) Early brain overgrowth in autism associated with an increase in cortical surface area before age 2 years. *Arch Gen Psychiatry* 68(5):467–476.
53. Carper RA, Moses P, Tigue ZD, Courchesne E (2002) Cerebral lobes in autism: Early hyperplasia and abnormal age effects. *Neuroimage* 16(4):1038–1051.
54. Kornack DR, Rakic P (1998) Changes in cell-cycle kinetics during the development and evolution of primate neocortex. *Proc Natl Acad Sci USA* 95(3):1242–1246.
55. Rippon G, Brock J, Brown C, Boucher J (2007) Disordered connectivity in the autistic brain: Challenges for the "new psychophysiology" *Int J Psychophysiol* 63(2):164–172.
56. Betancur C, Sakurai T, Buxbaum JD (2009) The emerging role of synaptic cell-adhesion pathways in the pathogenesis of autism spectrum disorders. *Trends Neurosci* 32(7):402–412.
57. Dalva MB, McClelland AC, Kayser MS (2007) Cell adhesion molecules: signalling functions at the synapse. *Nat Rev Neurosci* 8(3):206–220.
58. Lord C, Rutter M, Le Couteur A (1994) Autism Diagnostic Interview-Revised: A revised version of a diagnostic interview for caregivers of individuals with possible pervasive developmental disorders. *J Autism Dev Disord* 24(5):659–685.
59. Lord C, et al. (1989) Autism diagnostic observation schedule: A standardized observation of communicative and social behavior. *J Autism Dev Disord* 19(2):185–212.
60. Wechsler D (1999) *Wechsler Abbreviated Scale of Intelligence (WASI)* (Harcourt Assessment, San Antonio, TX).
61. Deoni SCL, et al. (2008) Standardized structural magnetic resonance imaging in multi-centre studies using quantitative T1 and T2 imaging at 1.5 T. *Neuroimage* 40(2):662–671.
62. Jovicich J, et al. (2006) Reliability in multi-site structural MRI studies: effects of gradient non-linearity correction on phantom and human data. *Neuroimage* 30(2):436–443.
63. Fischl B, Dale AM (2000) Measuring the thickness of the human cerebral cortex from magnetic resonance images. *Proc Natl Acad Sci USA* 97(20):11050–11055.
64. Dale AM, Fischl B, Sereno MI (1999) Cortical surface-based analysis. I. Segmentation and surface reconstruction. *Neuroimage* 9(2):179–194.
65. Fischl B, Sereno MI, Dale AM (1999) Cortical surface-based analysis. II. Inflation, flattening, and a surface-based coordinate system. *Neuroimage* 9(2):195–207.
66. Ségonne F, et al. (2004) A hybrid approach to the skull stripping problem in MRI. *Neuroimage* 22(3):1060–1075.
67. Kimmel R, Sethian JA (1998) Computing geodesic paths on manifolds. *Proc Natl Acad Sci USA* 95(15):8431–8435.
68. Sethian JA (1996) A fast marching level set method for monotonically advancing fronts. *Proc Natl Acad Sci USA* 93(4):1591–1595.
69. Worsley KJ, Andermann M, Koulis T, MacDonald D, Evans AC (1999) Detecting changes in nonisotropic images. *Hum Brain Mapp* 8(2-3):98–101.

SYSTEMS BIOLOGY